EFFECTS OF SCANNING STRATEGY ON RESIDUAL STRESS FORMATION IN ADDITIVELY MANUFACTURED TI-6AL-4V PARTS

Mohammad Masoomi[1], Scott M. Thompson[1,†], Nima Shamsaei[1], Meysam Haghshenas[2]

[1] Laboratory for Fatigue & Additive Manufacturing Excellence, Department of Mechanical Engineering, Auburn University, Auburn, AL, USA 36849

[2] Mechanical Engineering Department, University of North Dakota, Grand Forks, ND, USA 58202

† Corresponding author:
Email: smthompson@auburn.edu
Phone: (334) 844 4867

Abstract

Parts fabricated via directed energy additive manufacturing (AM) can experience very high, localized temperature gradients during manufacture. These temperature gradients are conducive to the formation of a complex residual stress field within such parts. In the study, a thermo-mechanical model is employed for predicting the temperature distribution and residual stress in Ti-6Al-4V parts fabricated using laser-powder bed fusion (L-PBF). The result is utilized for determining a relationship between local part temperature gradients with generated residual stress. Using this numerical model, the effects of scan patterns are investigated.

Introduction

Laser-Powder Bed Fusion (L-PBF) is an additive manufacturing (AM) method used for producing dense, metallic parts by way of melting successive layers of powder material by a laser. One of the challenges facing this method is residual stress formation and deformation of built parts [1,2]. Temperature gradients and cooling rates experienced during L-PBF can result in adverse material side effects such as residual stress or pore/defect formation, respectively [3,4]. There are different methods to evaluate the residual stress of the parts. In this study, neutron diffraction was employed to measure internal residual stresses at various locations along stainless steel (SS) 17-4 PH specimens additively manufactured via laser-powder bed fusion (L-PBF). Of these specimens, two were rods (diameter = 8 mm, length = 80 mm) built vertically upward and one a parallelepiped ($8 \times 80 \times 9$ mm^3) built with its longest edge parallel to ground. Simulations were performed using the commercially- available software COMSOL Multiphysics® 5.1 in conjunction with custom coding scripts.

Approach and Numerical Model

During the fabrication of part, powder will melt and solidify. To model transient heat transfer, numerical model was developed. The heat transfer in the part is governed by the heat equation:

$$\rho c_{\mathrm{i}}(\mathrm{T_i})|_{t_o-\Delta t} \left.\frac{\partial \mathrm{T_i}(x,y,z,t)}{\partial t}\right|_{t_o} = \nabla k_{\mathrm{i}}(\mathrm{T_i})|_{t_o-\Delta t} \nabla \mathrm{T_i}(x,y,z,t)\big|_{t_o} \quad (1)$$

where c_i is specific heat capacity and k_i is continuum thermal conductivity and ρ is the density. All modes of heat transfer, i.e. conduction, convection and thermal radiation, are taken into account in the model. The numerical model used in the study is developed by authors and explained in details at [5,6].

Since the local temperature gradient consists of three spatial components, i.e. parallel-to-track (x), perpendicular-to-track (y) and normal-with-substrate (z) directions, the magnitude of local temperature gradients was calculated herein. The magnitude of the temperature gradient (for a given time) between neighboring elements separated by $<\Delta x, \Delta y, \Delta z>$ was estimated using a second-order central difference, i.e.:

$$\|\nabla T\| \cong \left\| \left\langle \frac{T(x+\Delta x,y,z)-T(x-\Delta x,y,z)}{2\Delta x}, \frac{T(x,y+\Delta y,z)-T(x,y-\Delta y,z)}{2\Delta y}, \frac{T(x,y,z+\Delta z)-T(x,y,z-\Delta z)}{2\Delta z} \right\rangle \right\| \quad (2)$$

Process parameter chosen for this study is summarized in Table 1.

Table 1. Process parameters used for the experimental study

Substrate material	Ti-6Al-4V
Substrate size	10 x 10 x 1 cm^3
Powder description	Gas-atomized, air-dried
Powder layer thickness	30 μm
Powder bed porosity	0.4
Laser spot diameter	70 μm
Laser power	48 W
Laser wavelength	1075 nm
Scan speed	300 mm/s
Powder bed absorptance	0.25 [7]
Absorption coefficient	10^6 cm^{-1} [8]
Emissivity	0.35 [9]
Melt pool liquid thermal conductivity	25 – 45 W/m·K
Shielding gas type	Argon
Shielding gas temperature	20 ºC
Shielding gas flow rate	167 cm^3/s
Chamber wall temperature	20 ºC
Substrate temperature	20 ºC
Convection heat transfer coefficient	12.7 $W/m^2 \cdot K$

Numerical results and discussion

The size of the sample numerically investigated was 10 × 1 × 0.03 mm^3 and the PBF of the layer atop a previously-melted layer was simulated The tracks were unidirectional, meaning they went from right to left. The temperature and temperature gradient at the beginning, middle and end of a track are presented in Figure 1. It can be observed that temperature gradient decreases along the track.

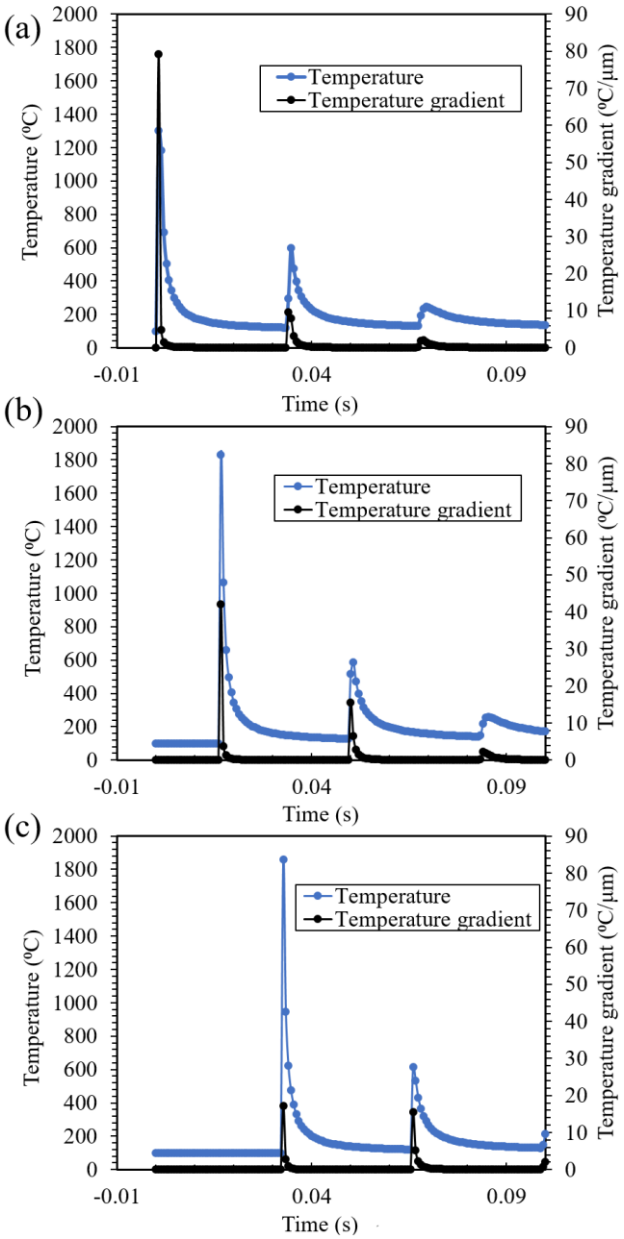

Figure 1. Temperature and temperature gradient at (a) start of track, (b) middle of track and (c) end of track.

The reason for lower temperature at the end of track can be attributed to heat accumulation effects. Since temperature gradients drive the formation of thermal stresses, it is reasonable to assume that higher temperature gradients will result in higher residual stresses and vice versa. Parry et al. [10] showed that residual stress decreases toward the end of a track during PBF. It is also important to investigate the effects of alternate scan strategy, instead of the unidirectional scan strategy. It is already presented that temperature gradient is highest at the start of track and will decrease significantly along the track. Using an alternate scan strategy, both ends would experience higher temperature gradient compared to middle of track. Based on these results, it is expected that temperature gradients would be higher near the surfaces of parts. Masoomi et al. [11] presented experimental residual stress data gathered from neutron diffraction.

Based on these data, when an alternating scan strategy is used, residual stress will be much higher near the surface as compared to the residual stress near the center.

Conclusions

In the study, the effects of thermal response on residual stress were studied. A framework to correlate thermal response to residual stress was provided. Effects of scan strategy on residual stress were studied. It was shown that temperature gradients and consequently residual stress will be lower at the end of a laser track relative to the beginning of it. It was concluded that using an alternating scan strategy will cause residual stress to be lowest at the center of parts and highest at both ends.

Acknowledgements

This work has been supported in part by NSF Grant #1657195.

References

[1] K. Dai, L. Shaw, Distortion minimization of laser-processed components through control of laser scanning patterns, Rapid Prototyp. J. 8 (2002) 270–276.

[2] B. Vrancken, V. Cain, R. Knutsen, J. Van Humbeeck, Residual stress via the contour method in compact tension specimens produced via selective laser melting, Scr. Mater. 87 (2014) 29–32. doi:10.1016/j.scriptamat.2014.05.016.

[3] C. Weingarten, D. Buchbinder, N. Pirch, W. Meiners, K. Wissenbach, R. Poprawe, Formation and reduction of hydrogen porosity during selective laser melting of AlSi10Mg, J. Mater. Process. Technol. 221 (2015) 112–120. doi:10.1016/j.jmatprotec.2015.02.013.

[4] A.M. Khorasani, I. Gibson, M. Goldberg, G. Littlefair, A survey on mechanisms and critical parameters on solidification of selective laser melting during fabrication of Ti-6Al-4V prosthetic acetabular cup, Mater. Des. 103 (2016) 348–355. doi:10.1016/j.matdes.2016.04.074.

[5] M. Masoomi, S.M. Thompson, N. Shamsaei, Laser powder bed fusion of Ti-6Al-4V parts: Thermal modeling and mechanical implications, Int. J. Mach. Tools Manuf. (2017) 73–90. doi:10.1016/j.ijmachtools.2017.04.007.

[6] M. Masoomi, X. Gao, S.M. Thompson, N. Shamsaei, L. Bian, A. Elwany, Modeling, simulation and experimental validation of heat transfer during selective laser melting, in: ASME, Houston, Texas, USA, 2015. doi:10.1115/IMECE2015-52165.

[7] P. Fischer, V. Romano, H.P. Weber, N.P. Karapatis, E. Boillat, R. Glardon, Sintering of commercially pure titanium powder with a Nd:YAG laser source, Acta Mater. 51 (2003) 1651–1662. doi:10.1016/S1359-6454(02)00567-0.

[8] Bert Huis in 't Veld, L. Overmeyer, M. Schmidt, K. Wegener, A. Malshe, P. Bartolo, Micro additive manufacturing using ultra short laser pulses, CIRP Ann. - Manuf. Technol. 64 (2015) 701–724. doi:10.1016/j.cirp.2015.05.007.

[9] S.S. Sih, J.W. Barlow, S. Sumin Sih, J.W. Barlow, S.S. Sih, J.W. Barlow, S. Sumin Sih, J.W. Barlow, The prediction of the emissivity and thermal conductivity of powder beds, Part. Sci. Technol. 22 (2004) 291–304. doi:10.1080/02726350490501682a.

[10] L. Parry, I.A. Ashcroft, R.D. Wildman, Understanding the effect of laser scan strategy on residual stress in selective laser melting through thermo-mechanical simulation, Addit. Manuf. 12 (2016) 1–15. doi:10.1016/j.addma.2016.05.014.

[11] M. Masoomi, N. Shamsaei, R.A. Winholtz, J.L. Milner, T. Gnäupel-Herold, A. Elwany, M. Mahmoudi, S.M. Thompson, Residual stress measurements via neutron diffraction of additive manufactured stainless steel 17-4 PH, Data Br. 13 (2017). doi:10.1016/j.dib.2017.06.027.